General Disclaimer

One or more of the Following Statements may affect this Document

- This document has been reproduced from the best copy furnished by the organizational source. It is being released in the interest of making available as much information as possible.

- This document may contain data, which exceeds the sheet parameters. It was furnished in this condition by the organizational source and is the best copy available.

- This document may contain tone-on-tone or color graphs, charts and/or pictures, which have been reproduced in black and white.

- This document is paginated as submitted by the original source.

- Portions of this document are not fully legible due to the historical nature of some of the material. However, it is the best reproduction available from the original submission.

Technical Memorandum 78107

X-Ray Spectra of Hercules X-I: III. Pulse Phase Dependence in High Energy Continuum

S. H. Pravdo, R. W. Bussard, R. H. Becker, E. A. Boldt, S. S. Holt, P. J. Serlemitsos, and J. H. Swank

MARCH 1978

National Aeronautics and Space Administration

Goddard Space Flight Center
Greenbelt, Maryland 20771

X-ray Spectra of Hercules X-1:
III. Pulse Phase Dependence in the High Energy Continuum

S.H. Pravdo*, R.W. Bussard*, R.H. Becker*, E.A. Boldt,
S.S. Holt, P.J. Serlemitsos, and J.H. Swank
Laboratory for High Energy Astrophysics
NASA/Goddard Space Flight Cneter
Greenbelt, Maryland 20771

ABSTRACT

We have observed pulse phase-dependent spectral changes in the high energy (> 20 keV) continuum of Hercules X-1. Cyclotron absorption of underlying continua can reproduce the observed angular dependence in the high energy cutoff. We discuss implications of this model, which include the possibility of determining the angular separation between the line of sight and the neutron star magnetic field if the absorbing electron spectrum is known.

*Also Dept. of Physics and Astronomy, Univ. of Maryland

I. INTRODUCTION

Hercules X-1 is an X-ray pulsar in a binary stellar system (Tananbaum et al. 1972). It exhibits a variety of temporal phenomena: 1.2-second pulsations, 1.7-day binary period, 35-day high-low cycle (cf. Giacconi et al. 1973; Davison and Fabian 1976)--and spectral features (cf. Clark et al. 1972; Ulmer et al. 1973; Holt et al. 1974; Becker et al. 1977; Pravdo et al. 1977a, Paper 1; Pravdo et al. 1977b, Paper 2). This communication reports on observations of Her X-1 performed by the Goddard Space Flight Center Cosmic X-ray Spectroscopy Experiment (CXS) on OSO-8 during August 31 - September 6, 1977. This was the second observation of the source with the CXS. A detailed study of the 2-20 keV spectrum of Her X-1 as a function of 1.2 second pulse phase was among the results (Paper 1) of the first observation in August 1975. Paper 1 reported the existence of a small region ($\sim$ 0.16) of pulse phase, asymmetrically located within the pulse peaks, in which the spectrum progressly hardens and then softens to its initial off-pulse value. We have extended this investigation by the use of a high energy CXS detector which is sensitive to X-rays between 2 and 60 keV. We report here pulse-phased spectroscopy > 20 keV, and demonstrate the consistency of all the 2-60 keV data with a cyclotron-absorbed X-ray source.

II. EXPERIMENT AND ANALYSIS

The detector is a multi-layer multi-anode xenon-filled proportional chamber with a mechanically collimated 5^{0} FWHM circular field of view (cf. Serlemitsos et al. 1976). It is pointed 5^{0} off the negative spin axis so that a 5^{0} cone is swept out during each satellite spin ($\sim$ 10 sec). The scan enables us to obtain a nearly simultaneous observation of the

diffuse X-ray background in the source free regions adjacent to Her X-1. The net Her X-1 spectrum is determined after subtracting off-source data from on-source data. Each pulse-height-analyzed (PHA) count is timed to within 20 msec. Thus an individual PHA count can be placed in its appropriate pulse phase bin after making time-of-flight corrections for the Her X-1 binary orbit, the satellite orbit, and the Earth's motion. The pulse period of 1.2377967 $\pm$ 0.0000004s (Pravdo et al. 1977c) has been divided into 62 temporal bins.

The method of spectral analysis has been presented elsewhere (Serlemitsos et al. 1975). In brief, an analytical model of the incident spectrum is multiplied by a previously determined detector response matrix. This resultant is then compared to the net PHA data using a χ^2 test. Once an acceptable fit is found, an inferred incident spectrum is obtained by dividing the PHA data by spectrum-dependent channel-by-channel efficiencies. In practice we have used a computer automated modification of the CURFIT subroutine described in Bevington (1969). This program yields estimates of errors on fitting parameters, which are close to one sigma errors whenever the "curvature" search option is used (Marquardt 1963). Unless otherwise stated these one sigma errors are presented. In other cases, the criteria discussed by Lampton et al. (1976) and Avni (1976) for increases in a minimum value of χ^2 are employed to determine parameter bounds with higher than one sigma confidence.

We have employed two basic models of the incident spectra for analysis. The first is a simple empirical model containing four parameters. It is of the form:

$$\frac{dN}{dE} \text{ (photons cm}^{-2}\text{sec}^{-1}\text{keV}^{-1}) = P_1 E^{-P_2} \quad \text{for } E \leq P_3$$

$$= P_1 E^{-P_2} \exp-\left(\frac{E-P_3}{P_4}\right) \quad \text{for } E > P_3.$$

This model serves in presenting the general trends of the spectra, but has no physical interpretation. The second model also contains an underlying power law spectrum with a high energy cutoff due to cyclotron absorption in a high ($\geq 10^{12}$ gauss) magnetic field (Daugherty and Ventura 1978). The physical parameters included in this model are the surface magnetic field strength, the angle between the line of sight and the magnetic field lines, the gravitational red shift, the polarization distribution of the X-rays, and a characteristic electron momentum, momentum spectrum, and column density of the absorbing electrons. Many of these parameters were held fixed at reasonable values (Section IV) so that in effect a three parameter model was fit (Section III).

III. RESULTS

In general there is excellent agreement with the results described in Paper 1. Figure 1 illustrates the Her X-1 pulse profile and spectral parameters in the simple empirical model as a function of pulse phase. The region of spectral hardening is well defined by the plot of spectral number index (Figure 1c). Phase zero of the pulse is defined to correspond to the bin in which the hardening reaches a maximum (i.e. number index reaches a minimum). Note that the high energy peak (> 25 keV) is asymmetric with respect to phase zero, and of greater phase duration than the hardened

region. This strongly supports the conclusion in Paper 1 that the intensity changes in the pulse are at most loosely connected to the spectral changes.

The power law index is determined and constrained largely by the low energy (< 15 keV) data. From the previous Her X-1 observation (Paper 1) we determined that the < 4.5 keV continuum in off-pulse spectra indicates a small amount of absorption by cold material. Also, when the flattened continua of the on-pulse spectra are extrapolated to energies below 4.5 keV, a low energy excess results. To avoid these complications data below 4.5 keV are not included in this analysis.

The final two plots in Figure 1 illustrate the cutoff parameters. "Off-pulse" bins are defined to be all bins with plus or minus phase greater than 0.08 (i.e. outside the hardened region). The off-pulse spectra have a lower cut off energy and higher e-folding energy than the on-pulse specta. This fact is quantitatively shown in Figure 2. The first two plots are a blow-up of the on-pulse high energy parameters. Also shown are the 99% joint confidence limits of these parameters determined from the combined off-pulse spectrum. In all cases, the model fits were acceptable with reduced chi squared (χ^2_R) $\sim$ 1 for $\sim$ 47 degrees of freedom. The net counts in these spectra range from 4 - 8000 for individual bins, to 175,000 for the combined off-pulse spectrum. The spectrum averaged over pulse phase has $E_{cutoff} = 19.5 \pm 0.3$ keV and $E_{folding} = 9.8 \pm 0.5$ keV in good agreement with the same parameters found by Becker *et al.* (1977).

The final Figure shows contrasting spectra, one from phase zero, and the other from an edge of the on-pulse region. We find no supporting

evidence for line emission near 60 keV (Trumper et al. 1978; Coe et al. 1977), although our one sigma upper limit is consistent with the line photon intensity observed by Trumper et al.

IV. DISCUSSION

The 1.2 second pulse period of Hercules X-1 identifies it as a neutron star. During stellar rotation, periodic views of an X-ray 'hot spot' create the observed pulsations. The X-ray energy source is the gravitational potential energy of accreting matter. Strong stellar magnetic fields constrain this matter to fall along field lines to the magnetic poles on the surface (Lamb et al. 1973). We suggest that the X-rays which comprise the spectrally hardened region of the pulse originate at the X-ray hot spot and are largely unaffected by scattering or absorption processes away from the hot spot (see also Paper I), in contrast to the X-rays observed at other pulse phases. Thus analysis of the hardened X-rays in this "spectrally defined beam" represents a deep probe in toward the neutron star surface.

It is clear that significant changes occur in the < 20 keV X-ray continuum of the above-mentioned beam. We leave discussion of this effect for a future work (Bussard and Pravdo 1978). In this discussion we will focus on the pulse-phase dependent changes in the > 20 keV continuum.

Boldt et al. (1976) showed that energy-dependent Compton scattering in a field of $\gtrsim 10^{13}$ gauss could reproduce the high energy cutoff. However the recent, lower estimates for the field strength (Trumper et al. 1978) taken together with the expected electron momenta distribution (see below), indicate that cyclotron absorption dominates over Compton scattering above 20 keV. In addition we consider the present model superior in that it

allows for the newly observed angular dependence in the cutoff. Cyclotron absorption is the inverse and co-existant process to cyclotron emission (Basko and Sunyaev 1975; Daugherty and Ventura 1977; Meszaros 1978) which may have been observed in the Her X-1 spectrum (Trumper et al. 1978).

The X-ray emitting region is located near the surface, so that the magnetic field does not change much from its surface value within the hot spot. The electron distribution here consists of infalling electrons and those which have been stopped by interactions in an accretion mound or atmosphere (Davidson 1973). High momentum electrons will observe continuum photons to be Doppler-shifted in the electrons' rest frames. If an electron momentum, P_e, satisfies the equation,

$$\frac{P_e}{mc} = -\left[\left(\left[\frac{2\beta}{B_q}-\left(\frac{E}{mc^2}\sin\theta\right)^2\right]^2-4\left[\frac{E}{mc^2}\sin\theta\right]^2\right)^{\frac{1}{2}}-\left(\frac{2\beta}{B_q}-\left[\frac{E}{mc^2}\sin\theta\right]^2\right)\cos\theta\right] \times\left[2\frac{E}{mc^2}\sin^2\theta\right]^{-1} \qquad (1)$$

then the electron resonantly absorbs the photon of energy E as a cyclotron line photon; where m is the electron rest mass and $B_q = \frac{m^2c^3}{e\hbar} = 4.414 \times 10^{13}$ gauss. The resulting X-ray spectrum has the form

$$\frac{dN}{dE}(\theta) = P_1 E^{-P_2} \exp\left[-N_e \sum_{\epsilon} f_\epsilon \sigma_c^\epsilon\right] \qquad (2)$$

where P_2 is the number index, N_e is the column density of electrons at the appropriate momentum $P_e(E,\theta)$, σ_c^ϵ is the cyclotron absorption

cross section (Daugherty and Ventura 1978) for polarization state ε, and f_ε the fraction in that state. We assume that the X-rays are unpolarized (Novick et al. 1977). Since the electrons are contrained to follow field lines, the angle θ is between the photon propagation direction (line of sight) and the polar field lines.

The magnetic field B in equation 1 must be between $2\text{-}7 \times 10^{12}$ gauss in this model. These limits are based on the observation that the high energy cutoff begins near 20 keV. If the magnetic field were smaller than 2×10^{12} Gauss then the cutoff would begin at much lower energies. A field larger than 7×10^{12} Gauss would require relativistic electrons for absorption of photons near 20 keV. We will not consider this possibility because other processes (e.g. pair production) become important in this regime. A value of 6×10^{12} gauss is adopted for B. This value is consistent with general theoretical estimates for a neutron star magnetic field (cf. Lamb 1974) and with direct (Trumper et al. 1978) and indirect (Paper 2) observational estimates. A gravitational redshift of 0.1 is assumed (cf. Middleditch and Nelson 1976).

The remaining critical parameters describe the absorbing electron distribution. We have chosen to let the angle θ be a free parameter for several electron distributions. This is illustrated in Figure 2c and 2d for an exponential electron momentum spectrum and a one-dimensional Maxwellian spectrum respectively. The spectra, with one exception, are acceptably fit by the model with $\chi^2_R = 0.9\text{-}1.4$ for 51 degrees of freedom. For the phase zero spectrum and the Maxwellian model, $\chi^2_R = 1.7$, because the model is more sharpely cutoff than the data. In all the models tested

the best fit values for θ perform a 10^0 - 20^0 excursion, with the angle of closest approach identified with phase zero. The actual values of the angles are strongly dependent on the column density of high momentum electrons. The low column density model (Figure 2c) could be appropriate if the absorbing electrons represent a small fraction of the total hot spot electrons--e.g. the infalling electrons. The high column density model (2d) could occur if all the electrons contribute to absorption. Basko and Sunyaev (1975), in a model for pulse formation, estimate that energy is deposited by infalling matter within 50 gm cm^{-2}. This yields an electron column density similar to those employed with the Maxwellian spectrum.

These column densities imply that the ranges of infalling particles are small enough ($\lesssim 10^3$ cm) so that the assumption of constant field strength is justified. In addition, estimates of the effective temperature of the hot spot ($\sim$ 30 keV) based on the X-ray continuum spectrum (Ulmer et al. 1972; Holt et al. 1974; Becker et al. 1977; this paper) yield a similar upper limit for the plasma scale height. The characteristic electron momenta in our models were chosen to be in this temperature range. The plots in Figure 2c and 2d are drawn for characteristic electron momentum P_0 = 180 keV/c, and the phase zero results for 160 keV/c and 200 keV/c are also included.

We note that the electrons which contribute to the absorption process have momenta as large as $\sim 4\ P_0$. These electrons on the exponential tail of the distributions have sufficient velocities to absorb $\gtrsim$ 20 keV photons in a field with a 60 keV characteristic line energy. Electrons with this high momentum can be created in knock-on collisions with infalling ions (Bussard and Ramaty 1978, Gamma Ray Spectroscopy in Astrophysics, proceedings of NASA/GSFC Conference, in preparation).

Off-pulse spectra have not been specifically addressed here. There are no obvious changes in spectral parameters over this region of pulse phase (Figure 1). We find that individual off-pulse spectra are acceptably fit by the best-fit model of the combined off-pulse spectrum with only the normalization left as a free parameter. This flux could be largely isotropic and originate from a Compton scattering shell of material at the Alfven surface (McCray and Lamb 1976; Basko and Sunyaev 1976; Ross et al. 1978).

This analysis can not unambiguously determine the separation between the line of sight and the magnetic field because the absorbing electron spectrum is unknown. A self-consistent model for the hot spot X-ray emission is needed. The gross variations in the continuum spectrum as a function of pulse phase (see Figure 1c) should be valuable in working backwards to the emitting electron spectrum. An improvement to the present model would consider the effects of re-emission which can be important in addition to absorption. This work is currently in progress (Bussard and Pravdo 1978).

Finally, we consider the implications of this analysis on the Her X-1 beaming mechanism. The beam is spectrally defined and the spectra in the beam indicate via parameterization that the angle of closest approach to the magnetic pole is at phase zero. A "pencil" beam is therefore favored. We note that the lower energy (< 20 keV) data alone could not have anticipated this model, and that all data 2-60 keV of which we are aware may now be consistently reconciled.

We thank J.L. Robinson-Saba and Dr. J.K. Daugherty for helpful discussions. We also thank Dr. M. Lampton for aid in parameter space.

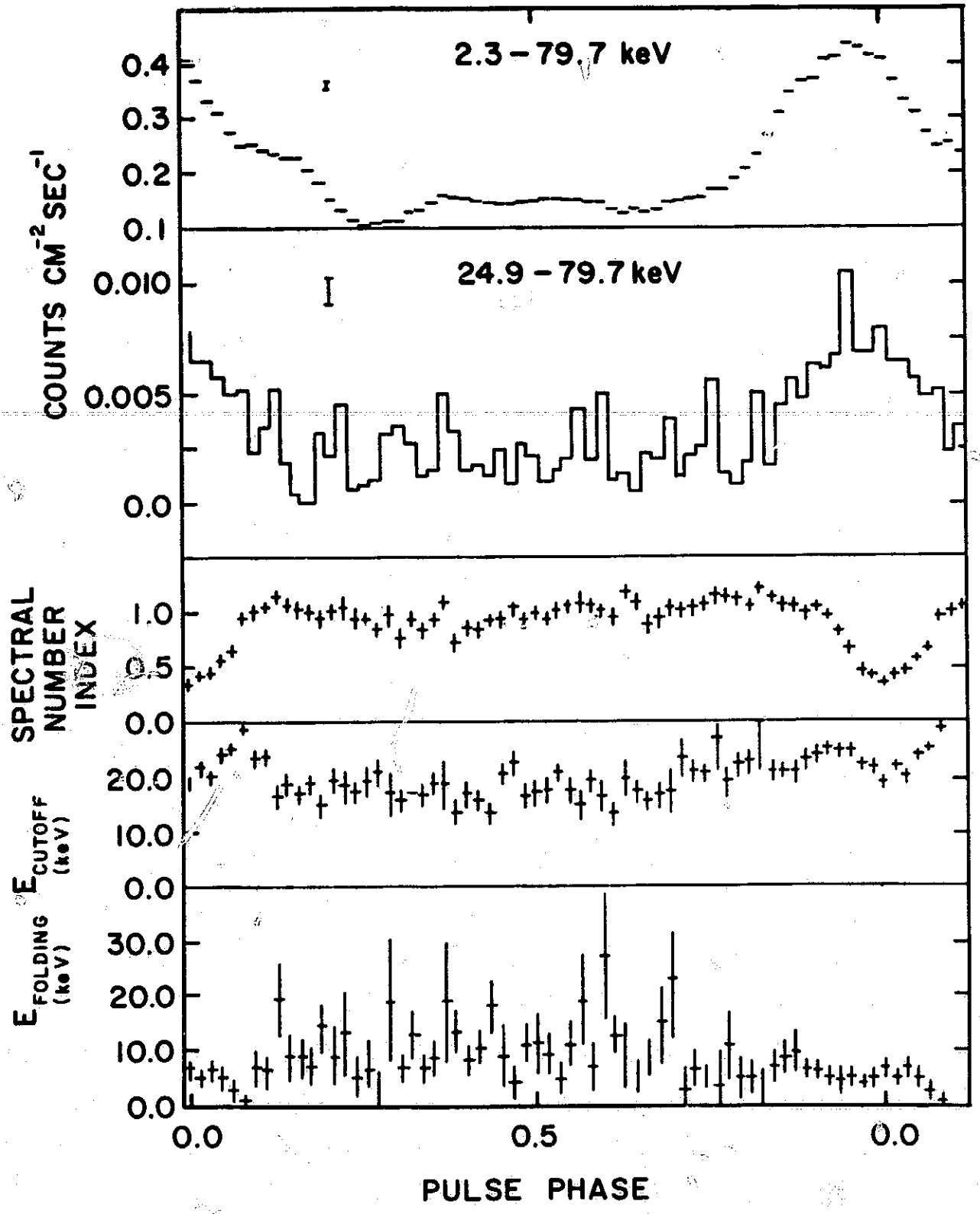
2.3 – 79.7 keV
24.9 – 79.7 keV
COUNTS CM^{-2} SEC^{-1}
0.4
0.3
0.2
0.1
0.010
0.005
0.0
SPECTRAL NUMBER INDEX
1.0
0.5
0.0
E_{CUTOFF} (keV)
20.0
10.0
0.0
$E_{FOLDING}$ (keV)
30.0
20.0
10.0
0.0
0.0
0.5
0.0
PULSE PHASE

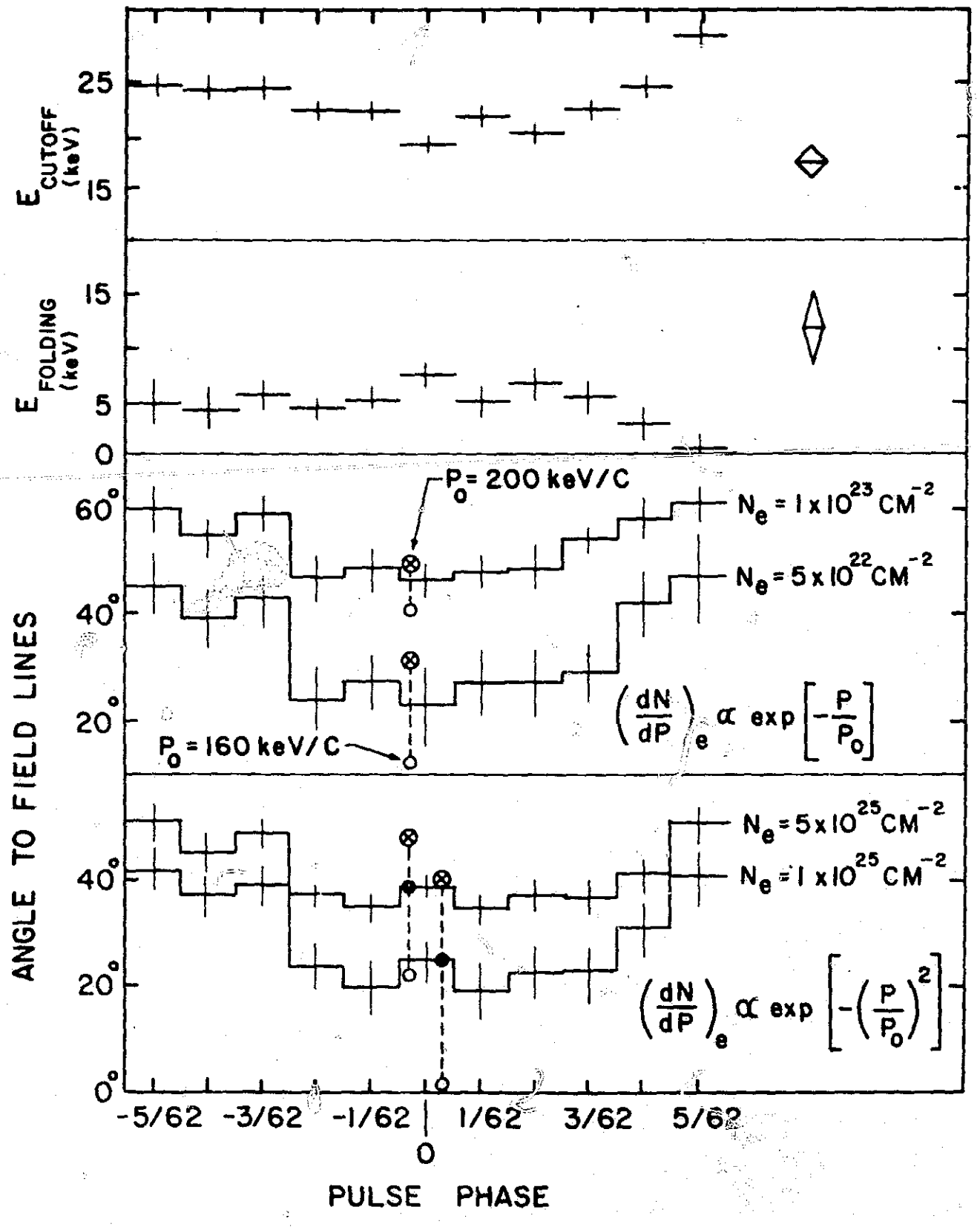
E_{CUTOFF} (keV)
25
15
$E_{FOLDING}$ (keV)
15
5
0
P_0 = 200 keV/C
$N_e = 1 \times 10^{23}\ CM^{-2}$
$N_e = 5 \times 10^{22}\ CM^{-2}$
P_0 = 160 keV/C
$\left(\frac{dN}{dP}\right)_e \propto \exp\left[-\frac{P}{P_0}\right]$
$N_e = 5 \times 10^{25}\ CM^{-2}$
$N_e = 1 \times 10^{25}\ CM^{-2}$
$\left(\frac{dN}{dP}\right)_e \propto \exp\left[-\left(\frac{P}{P_0}\right)^2\right]$
ANGLE TO FIELD LINES
60°
40°
20°
40°
20°
0°
-5/62 -3/62 -1/62 | 1/62 3/62 5/62
0
PULSE PHASE

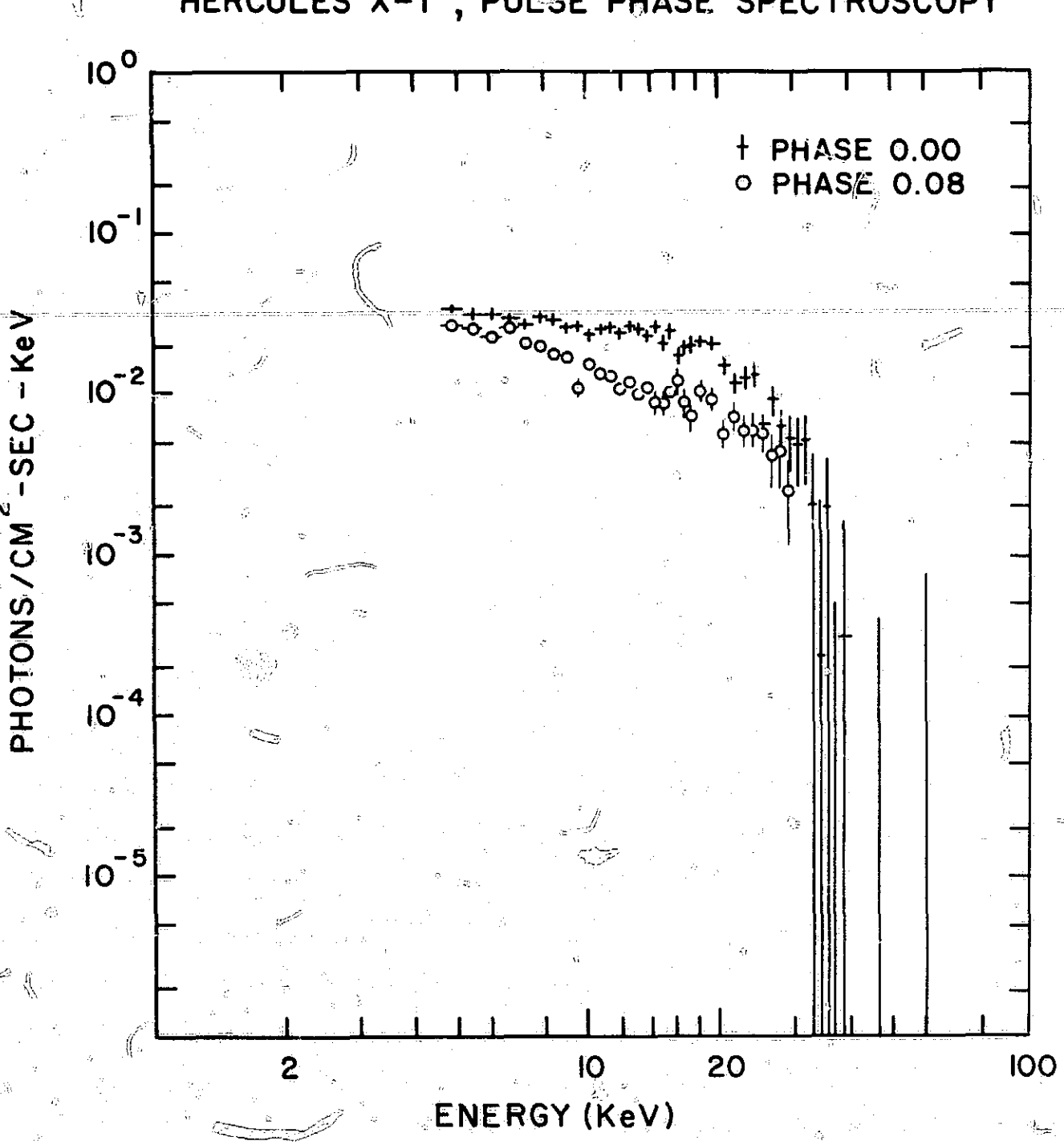
HERCULES X-1 , PULSE PHASE SPECTROSCOPY
PHASE 0.00
PHASE 0.08
PHOTONS/CM^2-SEC-KeV
10^0
10^{-1}
10^{-2}
10^{-3}
10^{-4}
10^{-5}
2
10
20
100
ENERGY (KeV)

REFERENCES

Avni, Y. 1976, Ap. J. 209, 16.

Basko, M. M. and Sunyaev, R. A. 1975, Astr. and Ap. 42, 311.

Basko, M. M. and Sunyaev, R. A. 1976, M.N.R.A.S. 175, 395.

Becker, R. H., Boldt, E. A., Holt, S. S., Pravdo, S. H., Rothschild, R. E., Serlemitsos, P. J., Smith, B. W., and Swank, J. H., 1977, Ap. J. 214, 879.

Bevington, P. R. 1969, Data Reducation and Error Analysis for the Physical Sciences, (McGraw-Hill Book Co., N.Y.), p. 237-9.

Boldt, E. A., Holt, S. S., Rothschild, R. E. and Serlemitsos, P. J. 1976, Astr. and Ap. 50, 161.

Bussard, R. W. and Pravdo, S. H. 1978, in preparation.

Clark, G. W., Bradt, H. V., Lewin, W.H.G., Markert, T. H., Schnopper, H. W., and Sprott, G. F. 1972, Ap. J. (Lett.) 177, L109.

Coe, M. J., Engel, A. R., Quenby, J. J., and Dyer, C. S. 1977, Nature 268, 508.

Daugherty, J. K. and Ventura, J. 1977, Astr. and Ap. 61, 723.

Daugherty, J. K. and Ventura, J. 1978, Phys. Rev D, in press.

Davidson, K. 1973, Nat. of Phys. Sci. 246, 1.

Davison, P.J.N. and Fabian, A. G. 1977, M.N.R.A.S. 178, 1P.

Giacconi, R., Gursky, H., Kellogg, E., Levinson, R., Schreier, E., and Tananbaum, J., 1977, Ap. J. 184, 227.

Holt, S. S., Boldt, E. A., Rothschild, R. E., Saba, J.L.R., and Serlemitsos, P. J. 1974, Ap. J. 190, L109.

Lamb, F. K. 1974, International Conference on X-rays in Space, U. of Calgary, Alberta, Canada.

Lamb, F. K., Pethick, C. J., and Pines, D. 1973, Ap. J. 184, 271.

Lampton, M., Margon, B., and Bowyer, S. 1976, Ap. J. 208, 177.

Marquardt, D. W. 1963, J. Soc. Ind. Appl. Math 11, 431.

McCray, R. and Lamb, F. K. 1976, Ap. J. (Lett.) 204, L115.

Meszaros, P. 1978, preprint.

Middleditch, J. and Nelson, J. 1976, Ap. J. 208, 567.

Novick, R., Weisskopf, M. C., Angel, J.R.P., and Sutherland, P. G. 1977, Ap. J. (Lett.) 215. L117.

Pravdo, S. H., Becker, R. H., Boldt, E. A., Holt, S. S., Serlemitsos, P. J. and Swank, J. H. 1977b, Ap. J. (Lett.) 215, L61.

Pravdo, S. H., Boldt, E. A., Holt, S. S., and Serlemitsos, P. J. 1977a, Ap. J. (Lett.) 216, L23.

Pravdo, S. H., Becker, R. H., Saba, J. R., Serlemitsos, P. J. and Swank, J. H. 1977c, IAU Circular No. 3116.

Ross, R. R., Weaver, R., and McCray, R. 1978, Ap. J. 219, 292.

Serlemitsos, P. J., Boldt, E. A., Holt, S. S., Rothschild, R. E. and Saba, J.L.R. 1975, Ap. J. (Lett.) 201, L9.

Serlemitsos, P. J., Becker, R. H., Boldt, E. A., Holt, S. S., Pravdo, S. H., Rothschild, R. E., and Swank, J. H. 1976, X-ray Binaries, NASA SP-389, p. 67.

Trumper, J., Pietsch, W., Reppis, C., Voges, W., Staubert, R., and Kendziorra, E. 1978, Ap. J. 219, L105.

Ulmer, M. P., Baity, W. A., Wheaton, W. A., and Peterson, L. E. 1973, Ap. J. (Lett.) 181, L33.

FIGURE CAPTIONS

FIGURE 1 a. The energy-integrated pulse light curve of Hercules X-1.

b. The high energy pulse light curve.

c.,d.,e. Spectral parameters in the empirical model for individual pulse bins.

FIGURE 2 a.,b. On-pulse spectral parameters in the empirical model. The diamonds are the 99% joint confidence limits for the parameters of the combined off-pulse spectrum.

c. Angle between the line of sight and the neutron star magnetic field versus pulse phase in the cyclotron absorption model. With an exponential electron momentum spectrum.

d. With a Maxwellian electron momentum spectrum.

FIGURE 3 Incident spectra of Hercules X-1 from minimum and maximum (absolute value) on-pulse phase.

1. Report No.	2. Government Accession No.	3. Recipient's Catalog No.
TM 78107		

4. Title and Subtitle	5. Report Date
X-ray Spectra of Hercules X-1: III. Pulse Phase Dependence in the High Energy Continuum	March 1978
	6. Performing Organization Code 661
7. Author(s) S.H. Pravdo, R.W. Bussard, R.H. Becker (U.MD.); S.S. Holt, P.J. Serlemitsos, J.H. Swank	8. Performing Organization Report No.
9. Performing Organization Name and Address E.A. Boldt Cosmic Radiations Branch Laboratory for High Energy Astrophysics Code 661	10. Work Unit No.
	11. Contract or Grant No.
	13. Type of Report and Period Covered TM
12. Sponsoring Agency Name and Address	14. Sponsoring Agency Code

15. Supplementary Notes

To be published in The Astrophysical Journal (Letters)

16. Abstract

We have observed pulse phase-dependent spectral changes in the high energy (> 20 keV) continuum of Hercules X-1. Cyclotron absorption of underlying continua can reproduce the observed cutoff in the high energy spectrum. We discuss this model which includes the possibility of determining the angular separation between the line of sight and the neutron star magnetic field if the absorbing electron spectrum is known.

17. Key Words (Selected by Author(s))	18. Distribution Statement

19. Security Classif. (of this report)	20. Security Classif. (of this page)	21. No. of Pages	22. Price*
U	U	16	

*For sale by the National Technical Information Service, Springfield, Virginia 22151.